Supplementary Information

Charge Carrier Trapping during Diffusion Generally Observed for Particulate Photocatalytic Films

Kenji Katayama[1*], Tatsuya Chugenji[1], Kei Kawaguchi[1]

1 Department of Applied Chemistry, Chuo University, Tokyo 112-8551, Japan;

*Corresponding authors:

K. Katayama, Phone: +81-3-3817-1913, E-mail: kkata@kc.chuo-u.ac.jp

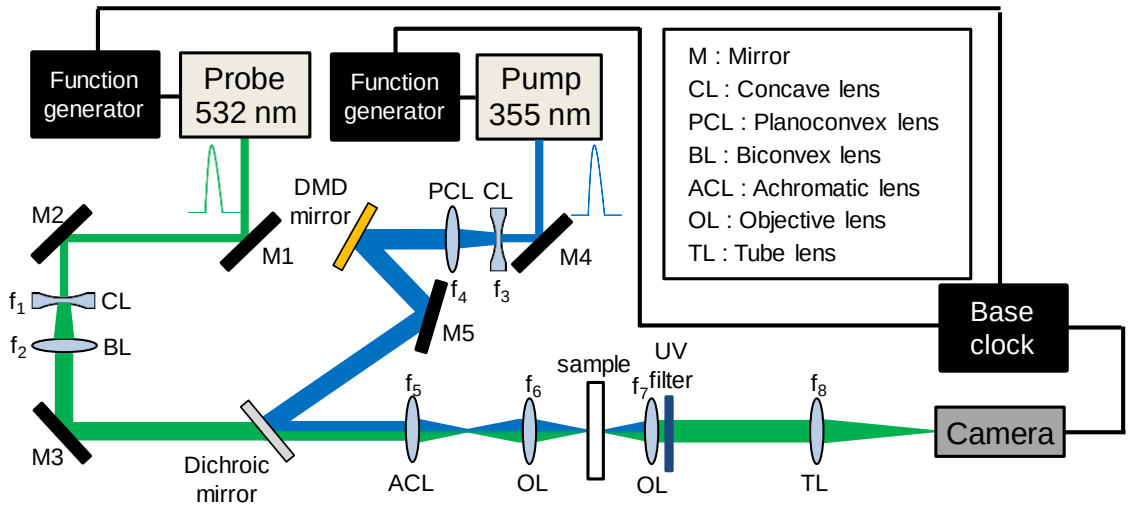

Fig. S1 Overview of the optical setup of the time-resolved pattern-illumination phase microscope is shown. The pump light was the third harmonics of an Nd:YAG pulse laser (pulse width: 5 ns, wavelength: 355 nm) (GAIA, Rayture Systems), and the probe light was the second harmonics of an Nd:YAG pulse laser (pulse width: 5 ns, wavelength: 532 nm) (GAIA, Rayture Systems). The pump pulse light was reflected by a digital micromirror device (DMD) (Light Crafter 4500, Texas Instruments), and the pattern was arbitrarily controlled by a computer. The image of the DMD mirror was relayed with a lens (f = 100 mm) and an objective lens (LMU-20X-NUV, Thorlabs) to irradiate the same pattern but reduced in size (1/14) onto a sample. The timing of these pulses was controlled by two function generators (WF1968, NF) triggered by a base clock (DF1906, NF). Each function generator controlled both the timing of the flash lamp and the Q-switch with a time resolution of 100 ps.

The pulsed illumination light was collimated with the pump light at a dichroic mirror and used to illuminate a sample. The transmitted light was imaged by an objective lens (LUCPLFLN20x, Olympus) with a working distance of 6.6-7.8 mm and a tube lens (TTL180-A. Thorlabs). A CMOS camera (MV1-D1024E-160, Photon Focus) with a sensor area of 10.9 mm x 10.9 mm (1024 x 1024 pixels) was used to obtain recordings. The central region in the vertical direction (200 x 1024 pixels) was recorded to reduce the computation burden. Each image was averaged 3-5 times, depending on the S/N ratio of the image, and it takes about 5-10 seconds for the acquisition of each image.

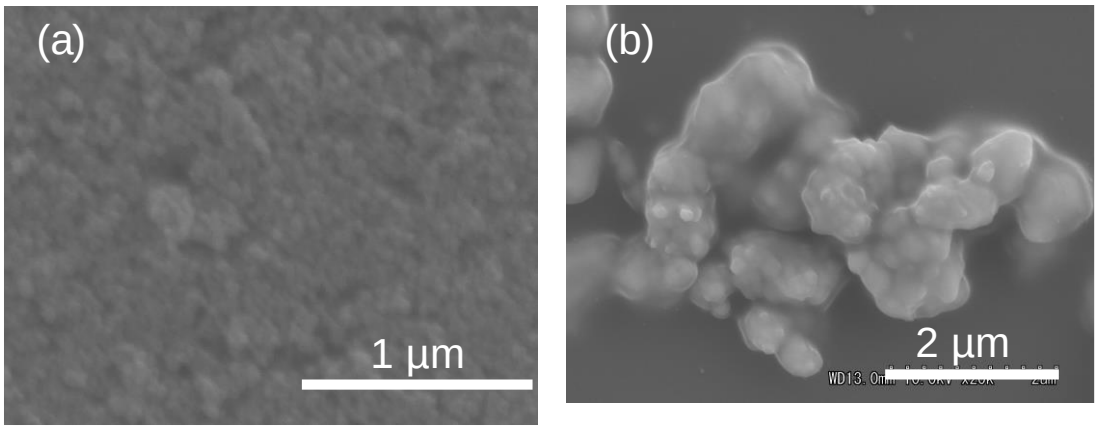

Fig. S2 The SEM images are shown for (a) TiO_2 particulate film, and (b) SrTiO3 particulate film, respectively.

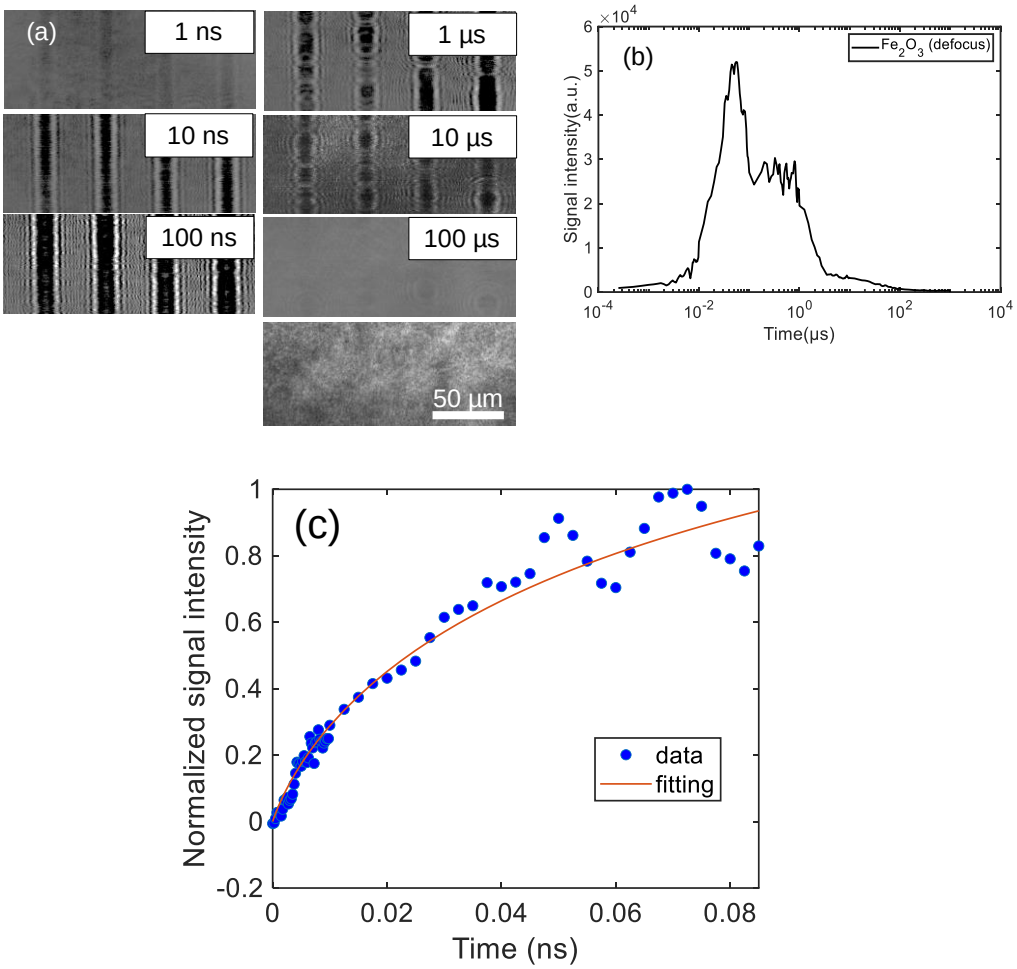

Fig.S3 The PI-PM image sequences for (a) a particulate film of hematite is shown. The sample images obtained under the same optical setup are also shown at the bottom of the sequence. (b) The normalized temporal responses of the refractive index change for the particulate film of hematite shown in (a) is shown. (c) The rising part of a hematite film and the fitting curve obtained from Eq. (4). The parameters were S=48.3 [-], β=1.63 [μm^{-1}], D_N=5.32 [$\mu m^2/\mu s$], respectively.

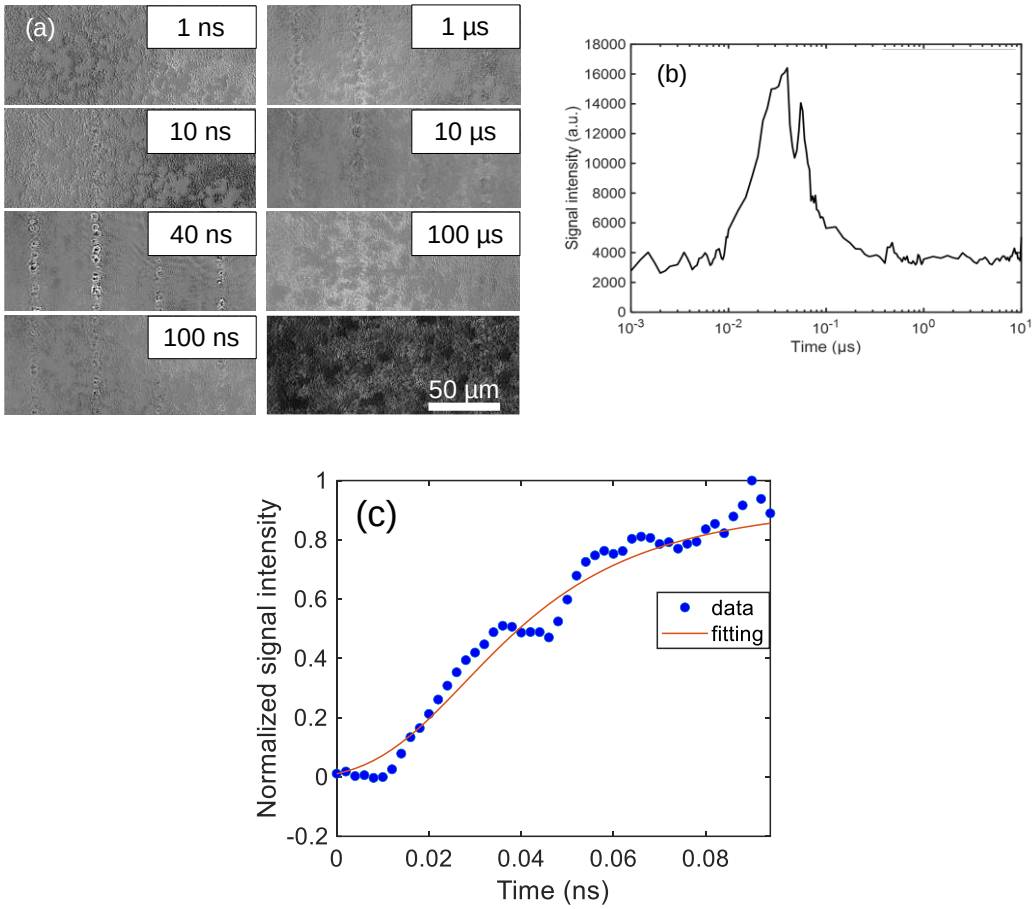

Fig.S4 The PI-PM image sequences for (a) a particulate film of $BiVO_4$ is shown. The sample images obtained under the same optical setup are also shown at the bottom of the sequence. (b) The normalized temporal responses of the refractive index change for the particulate film of $BiVO_4$ shown in (a) is shown. (c) The rising part of a $BiVO_4$ film and the fitting curve obtained from Eq. (4). The parameters were S=127 [-], β=10.1 [μm^{-1}], D_N=8.49 [$\mu m^2/\mu s$], respectively.

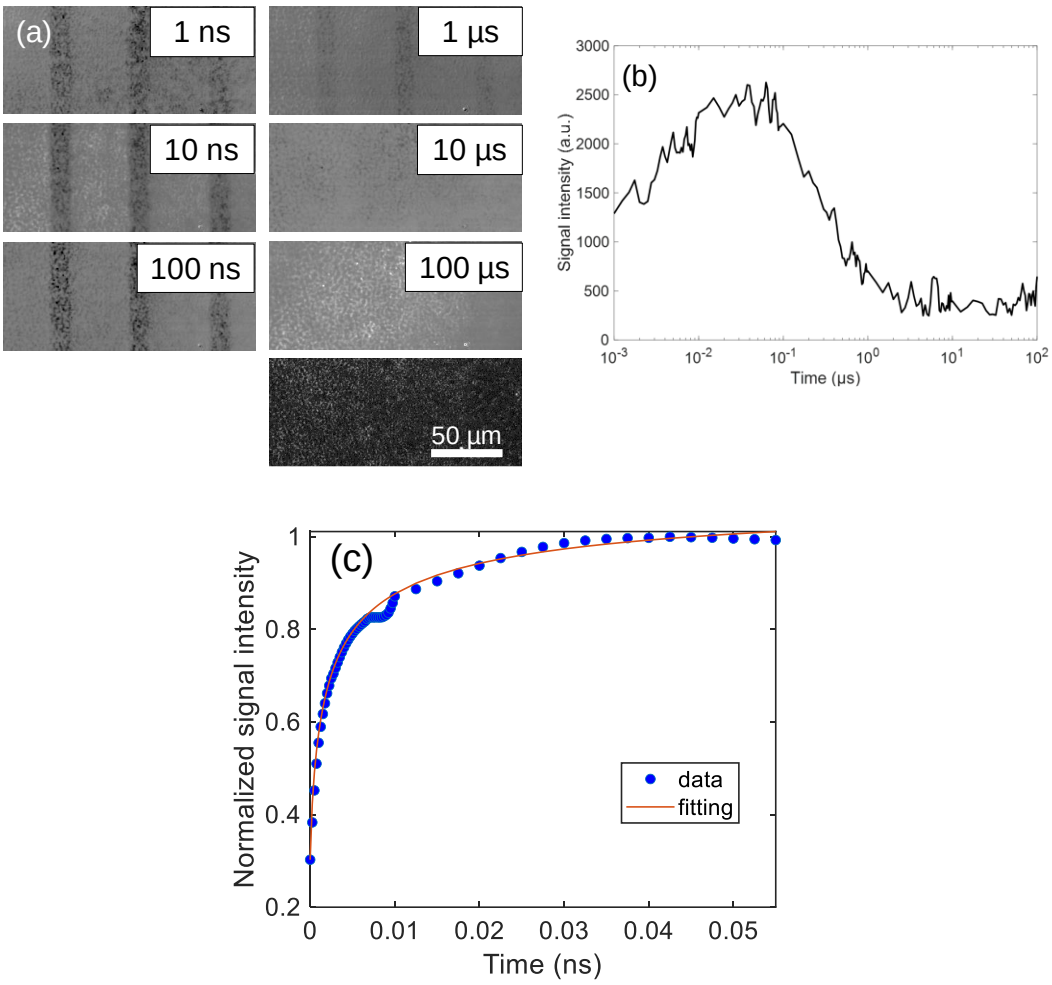

Fig.S5 The PI-PM image sequences for (a) a particulate film of methyl ammonium lead iodide (MAPI) is shown. The sample images obtained under the same optical setup are also shown at the bottom of the sequence. (b) The normalized temporal responses of the refractive index change for the particulate film of MAPI shown in (a) is shown. (c) The rising part of the MAPI film and the fitting curve obtained from Eq. (4). The parameters were S=127 [-], β=10.1 [μm^{-1}], D_N=8.49 [$\mu m^2/\mu s$], respectively.